PDTAC: Targeted photodegradation of GPX4 triggers Ferroptosis and potent antitumor immunity

Sijin Liu[1‡], Xi Zhao[1‡], Sufang Shui[1], Biao Wang[1], Yingxian Cui[1], Suwei Dong[1], Tairan Yuwen[1], Guoquan Liu[1 *]

[1] State Key Labaoratory of Natural and Biomimetic Drugs, School of Pharmaceutical Sciences, Peking University, Beijing, China

‡ These authors contributed equally to this work.

* Corresponding author, email: guoquanliu@bjmu.edu.cn

Abstract

Targeted degradation of proteins, especially those regarded as 'undruggable', attracts wide attention to develop novel potential therapeutic strategy. GPX4, a key enzyme regulating ferroptosis, is such a target whose inhibition is currently limited to molecules acting through covalently binding. Here, we have developed a targeted photolysis approach to achieve the efficiently degradation of GPX4. The Photo-Degradation TArgeting Chimeras (PDTACs) were synthesized by conjugating a clinically approved photosensitizer Verteporfin to GPX4-targeting peptides. Although the ligands themselves exhibit neither inhibitory nor degrading activity towards GPX4, these chimeras degraded selectively the target protein in living cells upon red-light irradiation. In contrast to the application of Verteporfin alone, the targeted photolysis of GPX4 resulted in dominant ferroptotic cell death in malignant cancer cells of different origins. Moreover, the dying cells resulted from our chimeras exhibited potent immunogenicity in vitro, and elicited more efficiently anti-tumor immunity in vivo in comparison with those dying from Verteporfin. Our approach therefore provides a novel method to dysfunction GPX4 based on noncovalent binding and specifically trigger immunogenic ferroptosis, which may boost the development of triggering ferroptosis as a potential strategy in cancer immunotherapy.

Ferroptosis, a regulated cell death driven by accumulation of lethal lipid peroxidation, has exhibited its potential physiological roles in T cell cancer immunotherapy and pathophysiological relevance as a therapeutic option in cancer treatment[1-5]. Glutathione peroxidase 4 (GPX4) plays a critical role in the ferroptotic cell death[6], and some therapy-resistant cancer cells are found to become vulnerable to GPX4 inhibition[2, 3]. Particularly, inhibiting GPX4 by RSL3 can result in immunogenic cell death (ICD) and induce efficient antitumor immunity as demonstrated recently in an in vivo tumor vaccination model[7]. However, targeting GPX4 by small-molecule inhibitors for cancer treatment remains challenging. The molecular surface of GPX4 lacks a drug-like binding pocket[8]. The canonic inhibitors (e.g. RSL3, ML210) all act through covalently bonding to the active site of GPX4 [6, 9, 10], which may suffer from low selectivity and undesired systemic toxicity for in vivo application[10-12].

Therefore, direct dysfunction of GPX4 through noncovalent binding is highly required for therapeutic considerations.

Motivated by the targeted photolysis methods of chromophore-assisted laser inactivation (CALI)[13, 14] and its variants[15-19], we aimed to develop Photo-Degradation TArgeting Chimeras (PDTAC) to selectively degrade GPX4 (Fig.1). These chimeras consist of three functional modules, a targeting ligand to bind the protein of interest (POI), a photosensitizer (PS) to generate reactive oxygen species (ROS) under light irradiation, and a linker to conjugate the previous two parts. As in photodynamic therapy (PDT), the ROS, particularly singlet oxygen ($^1O_2$), generated from PS react promiscuously with biomolecules including proteins[22]. The highly reactive $^1O_2$ exhibits short lifetime and diffusion distance, which restricts its effective range to tens of nm from where it is generated[20]. To utilize this localized reactivity, a targeting ligand that binds to the protein of interest (POI) can then direct most of the photo-induced $^1O_2$ to act on the target protein. With the highly reactivity of $^1O_2$ to oxidize amino acids or even to break the backbones, the POI could be then inactivated or even degraded[21, 22]. In principle, the three modules of PDTAC can be assembled to generate versatile molecules to degrade desired proteins. The coupling of protein degradation to light activation confers PDTAC highly spatiotemporal control, which would be highly beneficial for drug development.

In terms of therapeutical effect in cancer treatment, PDT with non-targeting PS usually results in complicated cell death modalities[23, 24]. This has usually hindered the control and the mechanistic understanding of the PDT triggered immunogenic activation[25]. In particular, Verteporfin (VPF), a clinically approved photosensitizer by FDA, has seldom been reported on its immunogenic activity despite of its wide use as PS in anticancer PDT studies[26]. Here, by conjugation of Verteporfin with GPX4-targeting ligands that exhibit neither inhibitory nor degrading activity, we have designed two PDTACs that selectively degrade GPX4 and dominantly induce ferroptotic cell death of potent immunogenicity.

Results and discussion

Synthesis and characterization of targeting chimers

We designed two new PDTAC molecules, consisting of VPF and a peptide targeting GPX4 (**PV-1** and **PV-2** in Fig.1). VPF, a clinically proved photosensitizer [23], was chosen because of its strong ability to generate singlet oxygen upon red-light irradiation that may readily degrade proteins. The two targeting peptides (**TP-1:** CRVDLQGWRRCRR and **TP-2:**CRAWYQNYCALRR), obtained using phage display technology, were previously reported to exhibit modest binding affinity towards GPX4 (K_D ~ μM) without inhibitory activity[27]. Based on the reported crystal structure of the peptide-GPX4 complexes[27], VPF was attached to the *N*-terminal of the peptides via a hydrophilic polyethyleneglycol (PEG) linker to mitigate hindrance on the binding with GPX4. Two PEG groups were used to reduce the distance from VPF to GPX4 to minimize the non-targeting effects of photo-induced ROS. Synthesis of these chimeras were achieved using the Fmoc-based solid phase peptide

synthesis (SPPS) (Fig.S1). In PBS/ACN (1:1) solution, absorption spectra and florescence spectra of the chimeras were similar to those of the VPF alone (Fig.S2b, S2d). Notably, the chimeras generate a large amount of $^1O_2$ upon light irradiation as detected by Electron Paramagnetic Resonance (Fig.S2e), comparable to VPF alone (Fig.2a). In PBS, the chimeras self-assembled into nanoparticles with the size of 20-30 nm measured by transmission electron microscope (TEM) (Fig.S3), driven by their amphipathic structure after the attaching of aromatic VPF. These particles are relatively stable with a zeta potential of +25 to +32 mV (Fig.S4b), due to the presence of multiple positive residues in the peptides. Accordingly, the fluorescence intensity and the ability to generate ROS of the chimeras in PBS were slightly lower than those of VPF (Fig.S2c, S2f).

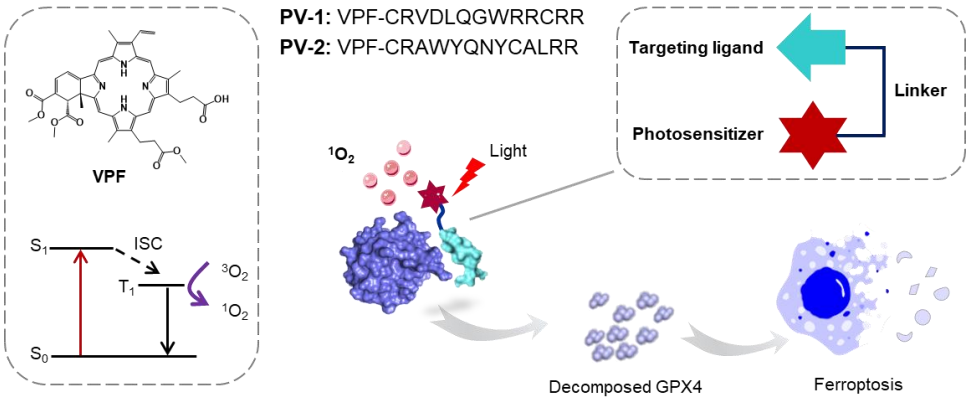

Figure 1. Schematic structure of the two PDTAC molecules and a cartoon description of the principle to photodegrade GPX4 and to trigger ferroptosis. A targeting ligand drives the chimera to bind with the protein of interest (not necessarily as an inhibitor). ROS (usually singlet oxygens) are generated from the photosensitizer upon light irradiation, and diffuse to degrade the GPX4 in proximity, which subsequently results in lipid peroxidation and ferroptosis.

We firstly checked whether these chimeras could penetrate cancer cells. The chimeras were incubated in A549 cells, a model for non-small cell lung cancer of medium sensitivity to ferroptosis, without using fetal bovine serum to enhance their cellular uptake. Confocal imaging based on the fluorescence of the VPF moiety showed that the two chimeras were readily taken up by A549 cells (Fig.2b). Interestingly, uptake rate of the chimeras was comparable to that of VPF alone as shown by flow cytometry, and 4 h incubation afforded a significant portion of chimeras inside the cells (Fig.S5). The high cellular uptake of these chimeras is not surprising. Their well-defined size of 20-30 nm and the presence of multiple positive amino residues (Arginine) are expected to facilitate their binding to the negative cancer cell membranes and the subsequent cellular internalization. This hypothesis is supported by the observation that PV-2 overlaps significantly with lysosomes while VPF does not (Fig.S5b). Moreover, the targeting ligand also drives PV-2 away from mitochondria on which a large portion of VPF enriches (Fig.S5c).

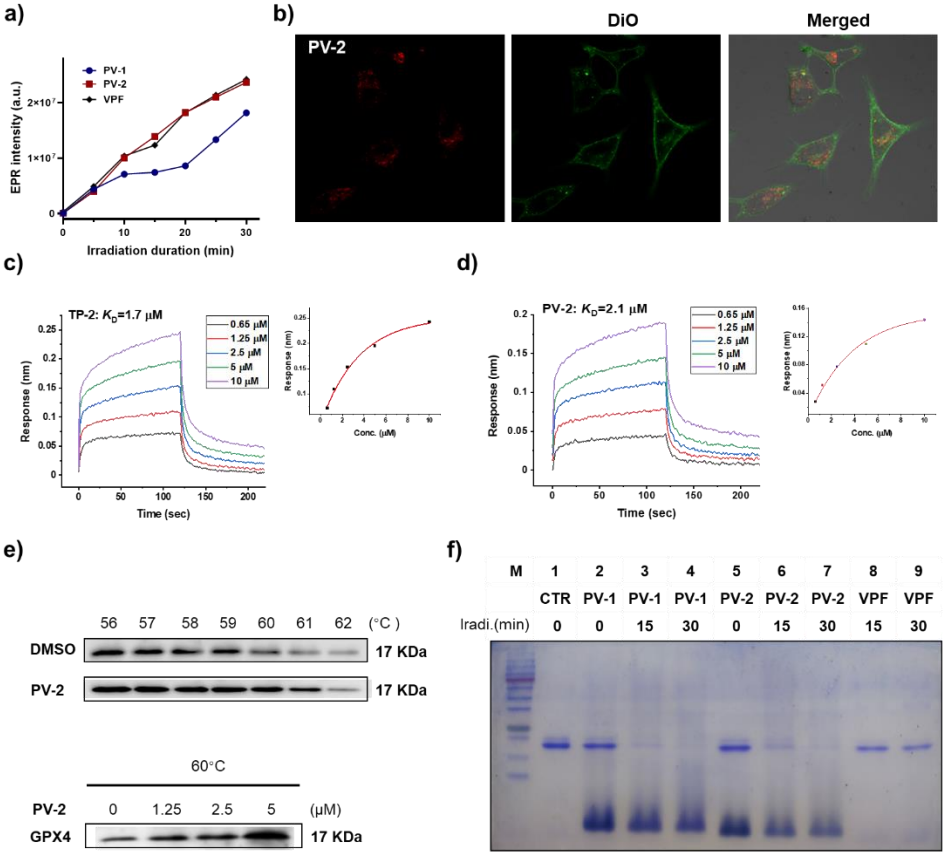

Figure 2. Characterization of the PDTAC molecules. a) The ability of chimeras to generate singlet oxygen upon light irradiation measured by EPR in PBS/ACN (1:1) solution (20 μM). 4-hydroxy-2,2,6,6-tetramethylpiperidine (4-OH-TEMP, 200 mM) was used as the spin trapper. b) Confocal imaging of the chimeras taken up by A549 cells after 15 h incubation. DiO was used to stain the membrane. c)-d) Measurement of the binding affinity of TP-2 (c) and **PV-2** (d) toward GPX4*mu* based on bio-layer interferometry. e) Cellular thermal shift assay of **PV-2** with GPX4 in A549 cells. Concentration of **PV-2** is 5 μM in temperature-dependent assays. f) Coomassie blue staining of GPX4*mu* in photolysis. Concentration of **PV-1**, **PV-2** and VPF is 10 μM. The SDS-PAGE analysis of lane 1-9 was then performed using 15% gel in SDS buffer at 200 V for 30 min. The irradiation in a) and f) was performed with a 300 W Xenon arc lamp (600 nm band-pass filter, 1.5 mW/cm^2) for designated duration.

To examine the binding affinity of these chimeras toward GPX4, recombinant GPX4 (Sec46Cys) mutant (hGPX4-C, Protein Data Bank entry 2OBI, abbreviated as GPX4*mu*) was expressed and purified[8, 28], which is appropriate for our studies because the targeting peptides bind to GPX4 in an area far from its active site (Sec46) [27]. Thermal shift assay based on differential scanning calorimetry (DSC) of intrinsic tryptophan fluorescence (ITF) showed a shift of T_m from 57 °C to approximately 61 °C after incubating GPX4*mu* with the chimeras or targeting peptides (Fig. S6). This significant shift suggests that the chimeras could bind to GPX4*mu*. Moreover, using bio-layer interferometry

(BLI), we found that both chimeras exhibited nearly unaffected affinity constant K_D compared to their parental targeting peptides, while VPF alone did not bind to GPX4*mu* (Fig.2c-2d, Fig. S7). These results demonstrate that not only the attachment of VPF did not affect the peptide-GPX4*mu* binding, but also the chimera nanoparticles could easily disassemble and subsequently bind to GPX4*mu*. According to the previous report, an intramolecular disulfide bond is formed in the GPX4*mu* complex with both targeting peptides[27]. To check whether this disulfide bond affects the binding affinity, we synthesized the corresponding refolded peptides and chimeras with an intramolecular disulfide bond. No difference in affinity constants was identified in the BLI measurements (Fig.S7). Therefore, the intramolecular disulfide bond is either not essential for the binding or it could be easily formed during its binding to GPX4.

Furthermore, we evaluated the targeted binding of chimera PV-2 towards GPX4 in living cells. Cellular thermal shift assay (CTSA) shows that PV-2 indeed increase the thermal stability of GPX4 (Fig.2e), consistent with the DSC based thermal shift assay with GPX4*mu* (Fig.S6). An effective concentration at μM scale is observed from the dose-dependent experiments (Fig.2e), which is comparable to its K_D obtained from BLI (Fig.2d). In sum, these findings demonstrate that PV-2 can not only efficiently penetrate the cell membranes, but also survive the cellular environment to retain its binding affinity towards GPX4 thereafter.

To test whether these chimeras could photodegrade GPX4*mu*, we used Bradford protein assay based on Coomassie blue to monitor the photolysis process. Both chimeras could nearly eliminate the GPX4*mu* band in SDS-PAGE analysis after 15-min irradiation (Fig.2f), while VPF alone exhibited just medium effect on GPX4*mu*. These results prove principally our designed idea that the targeting peptides direct the photo-induced ROS to efficiently degrade the protein of interest.

Selective photolysis of GPX4 in cellular lysate

Because PDTAC can directly degrade proteins through photo-induced ROS, cellular pathways (e.g. the proteasomal and lysosomal system) should be dispensable. We therefore examined whether photo-irradiation of these chimeras could degrade GPX4 in cellular lysate. After mixing the chimeras with A549 lysate for approximately 60 min using a reciprocating shaker, the lysate mixture was irradiated by a Xenon lamp. The proteins were then collected and analyzed by western blot right after the irradiation to minimize any involvement of cellular pathways. Both chimeras could significantly degrade GPX4 when exposed to light for 5 min and exhibited an obvious concentration dependence (Fig.3a, 3c, 3f). Furthermore, the degradation of GPX4 was also dependent on the irradiation duration when the chimera concentration was fixed (Fig.3b, 3d). The GPX4 level was not affected at all without light irradiation, indicating the degradation occurs as a consequence of photo-induced ROS. Interestingly, such a degradation is highly selectively while the abundance of GPX1, another member of the GPXs family, remained unaffected (Fig.3e). Additionally, other proteins, e.g., ACSL4 (a negative regulator of ferroptosis[29]), ACAT1 (regulating sterol metabolism), were also not affected under the same treatment (Fig.3e).

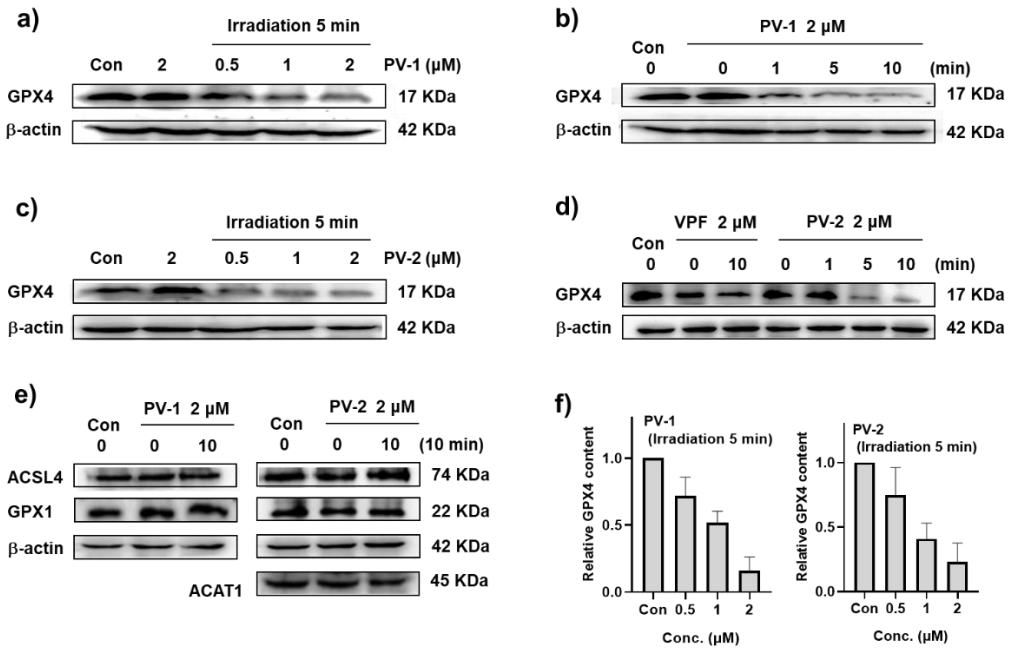

Figure 3. Selective degradation of GPX4 by **PV-1** and **PV-2** in cellular lysate. The degradation exhibits concentration dependence (a, c) and time dependence (b, d). **PV-1** and **PV-2** treatments did not degrade proteins other than GPX4 (e). (f) Relative GPX4 content obtained in three independent experiments. Light irradiation was performed using a Xenon lamp with a 600 nm band-pass filter (~1.5 mW/cm^2) for designated duration. Proteins were immunoblotted with their corresponding antibodies.

Selective photolysis of GPX4 in living cells

Since our CTSA shows that PV-2 effectively engages with GPX4 in living cells (Fig.2e), we then investigated whether these chimeras retained their ability to photodegrade GPX4 in the complex cellular environment. As expected, GPX4 was also degraded by irradiation of either **PV-1** or **PV-2**, depending on both the irradiation duration and the chimera concentrations (Fig.4a-d). The similar observation that chimeras without light irradiation did not affect the GPX4 level confirmed again the key role of photo-induced ROS in this living cell protein degradation. Examination on the abundance of other proteins including ACSL4, GPX1 and ACAT1, also demonstrate the selectivity of the photolysis by **PV-1** and **PV-2** (Fig. 4e). In contrast, the targeting peptides alone, either with or without light irradiation, did not affect the GPX4 abundance (Fig. 4a-d, Fig.4g-h). This is consistent with the previous report that they only bind to GPX4 without any inhibitory activity[27]. Moreover, we used Coomassie blue to stain the whole cellular proteins in SDS-PAGE to examine the selectivity of photodegradation. Interestingly, color fading in the band corresponding to GPX4 was observed in the PV-2 treated cells, while other bands are similar to those in the untreated cells (Fig. 4f).

Because of its non-targeting nature, the VPF alone is expected to exert its degradation ability over

various proteins. In cellular lysate, photolysis of GPX4 by VPF was not as significant as that by **PV-1** and **PV-2**, while other proteins including GPX1 and ACSL4 could be also degraded to some extent by VPF (Fig. S8). In living cells, VPF could also simultaneously degrade several proteins including GPX1, GPX4, ACSL4 and ACAT1 (Fig.S9). Particularly, at higher VPF concentrations (e.g., 5 μM) with 5-min irradiation, all the proteins examined in our experiments were nearly depleted. These results demonstrate the non-selective nature of the photolysis by VPF. Therefore, the selective photolysis of GPX4 by **PV-1** and **PV-2** is ascribed to presence of the targeting ligands, which direct the photo-induced ROS mainly to degrade GPX4.

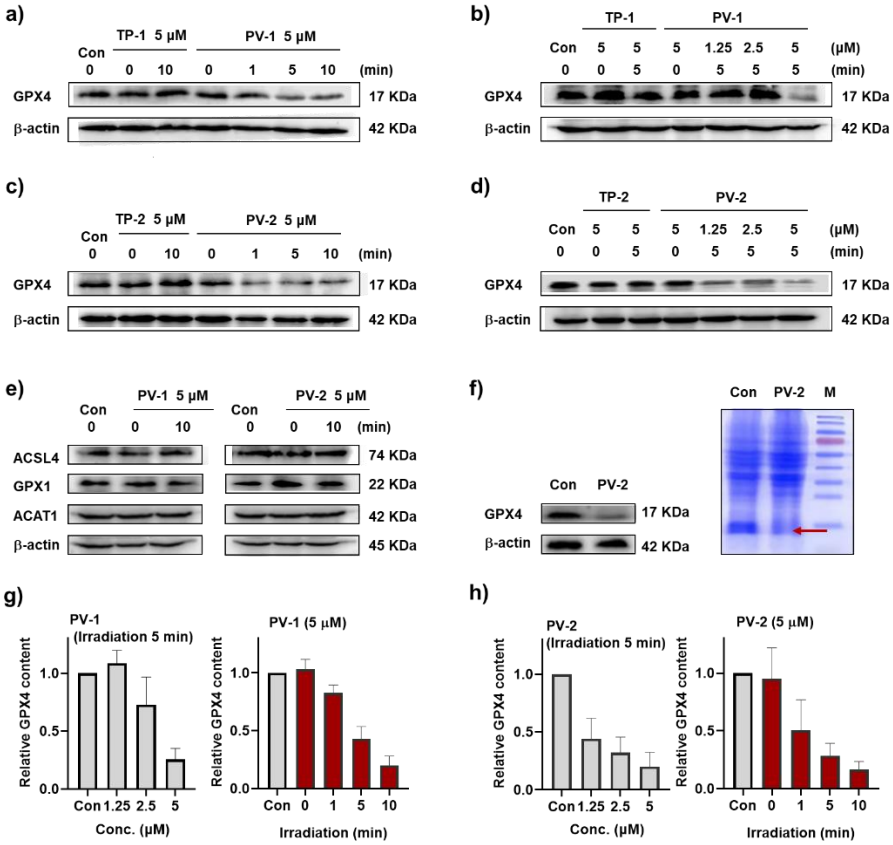

Figure 4. Selective degradation of GPX4 by **PV-1** and **PV-2** in living A549 cells. The photodegradation exhibits concentration dependence (a, c) and time dependence (b, d). Treatment with the targeting peptides alone could not degrade GPX4 (b, d), and treatments with **PV-1** or **PV-2** did not degrade proteins other than GPX4 (e). f) Comparison of whole proteins in SDS-PAGE analysis based on Coomassie blue staining after photolysis (concentration of **PV-2** is 5 μM). The red arrow denotes the position of GPX4 where a shallower band was observed in the **PV-2** treated cells. (g)(h) Relative GPX4 content obtained in three independent experiments. For all photolysis, light irradiation was performed using a Xenon lamp with a 600 nm band-pass filter (~1.5 mW/cm^2) for designated duration.

Photolysis of GPX4 induces dominantly ferroptosis

PDT usually induces multiple cell death modalities in cancer treatment[24, 25], because of the intrinsically non-targeting nature of photo-induced ROS. Previous targeting photosensitizers used

in PDT were designed to selectively increase their accumulation in tumor cells[30], but the cell death was still induced dominantly by random damages from photo-induced ROS. Particularly, we have recently found that the concentration of PS and light luminance could tune the cell death modalities in PDT[31].

As a key regulator of Ferroptosis, GPX4 reduces phospholipid hydroperoxides (PLOOHs) to the corresponding alcohols (PLOHs)[32, 33], and its degradation would trigger lipid peroxidation. Using C11-BODIPY as a probe, elevated lipid peroxidation was detected in **PV-1** treated cells after light irradiation (Fig.S10a). We then evaluated the cell death in A549 cell lines (Fig.S10, Fig.S11), and in cancer cells highly sensitive to Ferroptosis, e.g., triple-negative breast cancers (MDA-MB-231, 4T1) and melanoma (murine B16) (Fig.5). Lip-1, a specific inhibitor of lipid peroxidation, can effectively blocked the ferroptotic cell death[11]. Indeed, we observed that Lip-1 not only decreased the lipid ROS level, but also rescued the cell death caused by PDT with both chimeras (Fig.5b, Fig.S10). Two other Ferroptosis inhibitor, the iron chelator deferoxamine (DFO) and the ACSL4 inhibitor rosiglitazone (ROSI), could also significantly rescue the cell death triggered by these chimeras (Fig.5c, Fig.S10-S11). Moreover, necrotic cell death is usually the main cell death pathway under high PS concentration. PDT with 4-5 μM VPF resulted in quick disruption of cell membrane shown by trypan blue staining, while cells treated by the two chimeras were still intact (Fig. 5d, Fig.S12). Consistently, this cell death caused by VPF treatment could be rescued neither by Lip-1 nor the iron chelator DFO (Fig.5b-5c, Fig.S12).

We have previously identified a distinct cell death pathway featuring also elevated lipid peroxidation (termed as Liperoptosis) in PDT with non-targeted PS[31]. In Liperoptosis, the lipid peroxidation results from non-enzymatic oxidization of lipids, and therefore it is independent of ACSL4 and could not be rescued by DFO. Therefore, the cell death triggered by the two chimeras, which could be effectively rescued by both an ACSL4 inhibitor and DFO (Fig.5c, Fig.S10), is different from the Liperoptosis triggered by non-targeted PS. Admittedly, multiple cell death pathways may be still present, as neither Ferroptosis inhibitors completely blocked the cell death by the chimeras. Off-target effects of these chimeras are still present to some extent, which is indicated by the increase of cellular ROS assessed by DCFH (Fig.S10e).

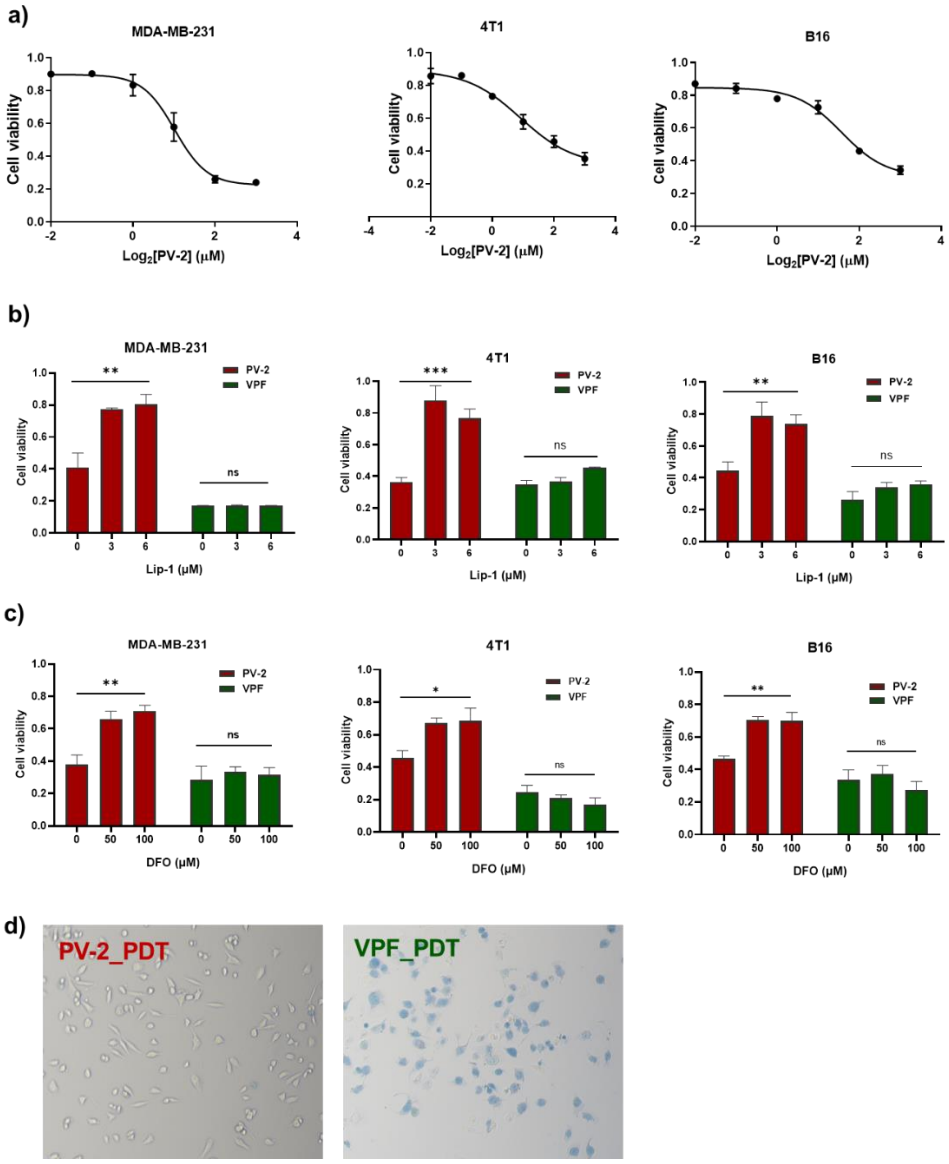

Figure 5. PDT with **PV-2** induces ferroptosis in multiple cancer cells. a) Dose dependence of cell viability on **PV-2** under PDT irradiation. b) Ferroptosis inhibitor Lip-1 significantly rescue the death caused by PDT with **PV-2**, but not those by PDT with VPF (4 μM for 3 min × 2 irradiation). c) Iron chelator DFO significantly rescued the cell death caused by PDT with **PV-2**, but not those by PDT with VPF (4 μM for 3 min × 2 irradiation). d) Trypan blue staining showed disrupted plasma membranes in MDA-MB-231 cells 30 min after PDT with **PV-2** or VPF (4 μM for 2 min irradiation). PDT was performed using a Xenon lamp with a 600 nm band-pass filter (~1.5 mW/cm^2) for designated duration. Data were typically plotted as the mean ± s.d. (n = 3). The statistical differences were calculated by a Student's *t*-test (*p<0.05, **p<0.01, ***p<0.001).

Photolysis of GPX4 triggers potent immunogenic cell death

Ferroptosis, especially that triggered by RSL3, has been found to be immunogenic due to the release of damage-associated molecular patterns (DAMPs)[7, 34]. By selectively degrading GPX4, our targeted photolysis strategy specifically drove cancer cells to undergo ferroptosis, and therefore we

expected it to elicit efficient immunogenicity. By vaccinating immune-competent mice with **PV-2** treated dying cancer cells, efficient antitumor immunity was observed based on the elongated surviving rate and the delayed tumor growth when the mice were re-challenged with viable cancer cells (Fig.6a-6c). PDT with some non-targeted PSs can be also immunogenic[35]. We found indeed that VPF showed obvious effect in both surviving rate and tumor growth delay experiments (Fig.6b-6c). However, **PV-2** outperforms VPF in both experiments, pointing to the important role of GPX4 degradation in immunogenic activation. Consistently, in vitro stimulation of murine BMDCs demonstrated that **PV-2**-treated cancer cells resulted in more potent BMDC maturation than VPF treated cells as revealed by expression level of MHC II and CD86 in $CD11c^+$ BMDCs (Fig.6f-6g). This trend was observed over different PS concentrations, irradiation times and different BMDC/B16 ratios (Fig.S13), demonstrating the superior performance of **PV-2**. Measurement of released ATP and HMGB1 from the dying cancer cells also showed that **PV-2** treatment induced higher concentrations of these two common DAMPs (Fig.6d-6e).

Although PDT could trigger ICD, many factors may complicate its practical application in cancer immunotherapy[36]. The efficiency of PDT to induce ICD depends largely on the nature, the concentration of photosensitizers, as well as the illuminance density. For instance, VPF, as a FDA approved photosensitizer with red right absorption, only triggers weak ICD (Fig. 6) and exhibited strong concentration dependence (Fig.S13). In contrast, our GPX4-targeted photosensitizers, particularly **PV-2**, induce much more potent ICD and result in more efficient anti-tumor immunity in vivo (Fig.6). These results demonstrate the superiority and potential clinical values of inducing a well-defined cell death modality by PDT in cancer immunotherapy.

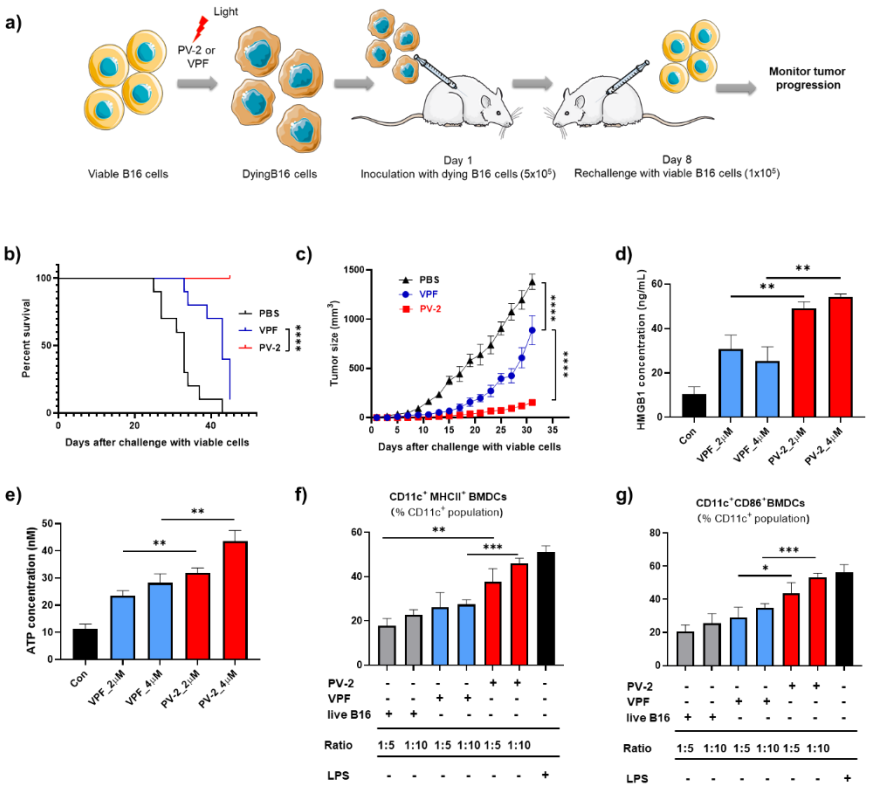

Figure 6. PDT with **PV-2** induces immunogenic cell death both in vitro and in vivo. a) The in vivo prophylactic tumor vaccination model. b) Kaplan-Meier surviving curve of the mice challenged with variable B16 cells after vaccination with VPF or **PV-2** treated dying B16 cells. c) The tumor size at the challenge site of the mice in the prophylactic tumor vaccination model. Data were plotted as the mean ± s.d. (n = 10). d) HMGB1 release from the B16 cells treated with PDT using VPF or **PV-2**. e) ATP release from the B16 cells treated with PDT using VPF or **PV-2**. f) and g) B16 cells treated with PDT using VPF or **PV-2** induces maturation of BMDCs. LPS (100 ng/mL) was used as a positive control. Irradiation was performed using a Xenon lamp with a 600 nm band-pass filter (~1.5 mW/cm^2) for designated duration. Data were typically plotted as the mean ± s.d. (n = 3) unless specified. The statistical differences in the Kaplan-Meier curve were calculated by a log-rank (Mantel-Cox) test, and were calculated by a Student's *t*-test in other cases (*p<0.05, **p<0.01, ***p<0.001).

This selective photodegradation of proteins through PDTAC, shares some features of the fast-emerging PROTAC (PRoteolysis TArgeting Chimera) technology[37-39]. The photolysis of GPX4 well demonstrates at least two features of them, the use of non-inhibitory targeting ligands and particularly the degradation of "undruggable" protein target. Moreover, the PDTAC inherits high spatiotemporal precision of light activation, which may help reduce systemic toxicity when used in vivo. Additionally, the versatile options of photosensitizers can lead to photolysis using near-infrared light, an optimal condition for in vivo application. Admittedly, more studies, e.g., optimizing both the targeting ligands and photosensitizers, are definitely required to fully demonstrate the advantages of PDTAC in targeted protein degradation. Particularly, expanding the targeting ligand to small molecules is currently under investigation.

Conclusions

To conclude, we have proposed a distinct strategy PDTAC composed of three replaceable modules to induce photodegradation of proteins. To demonstration its feasibility, we synthesized two targeting chimeras by conjugating a peptide ligand without inhibitory activity to the photosensitizer, aiming to trigger ferroptosis in cancer cells based on targeted degradation of GPX4. These chimers retain the binding affinity toward GPX4 and selectively degraded GPX4 in both cellular lysate and living cells upon red-light irradiation. Photodegradation of this enzyme could induce lipid peroxidation, and dominantly switch the cell death to ferroptosis, which triggers potent immunogenic reactivity both in vitro and in vivo. Our targeted degradation of GPX4 based on the PDTAC strategy provide a novel light-activable method for induction of ferroptosis, which may boost its application in cancer immunotherapy.

Acknowledgement

G.L. acknowledges the financial support from the National Natural Science Foundation of China

(22177008, 91643112), the National Key R&D Program of China (2018YFC0115003), and We thank Dr. Jing Wang of the State Key Laboratory of Natural and Biomimetic Drugs for BLI measurements.

References

1. Dixon, S. J.; Lemberg, K. M.; Lamprecht, M. R.; Skouta, R.; Zaitsev, E. M.; Gleason, C. E.; Patel, D. N.; Bauer, A. J.; Cantley, A. M.; Yang, W. S.; Morrison, B., III; Stockwell, B. R., Ferroptosis: An Iron-Dependent Form of Nonapoptotic Cell Death. *Cell* **2012,** *149* (5), 1060-1072.

2. Hangauer, M. J.; Viswanathan, V. S.; Ryan, M. J.; Bole, D.; Eaton, J. K.; Matov, A.; Galeas, J.; Dhruv, H. D.; Berens, M. E.; Schreiber, S. L.; McCormick, F.; McManus, M. T., Drug-tolerant persister cancer cells are vulnerable to GPX4 inhibition. *Nature* **2017,** *551* (7679), 247-+.

3. Viswanathan, V. S.; Ryan, M. J.; Dhruv, H. D.; Gill, S.; Eichhoff, O. M.; Seashore-Ludlow, B.; Kaffenberger, S. D.; Eaton, J. K.; Shimada, K.; Aguirre, A. J.; Viswanathan, S. R.; Chattopadhyay, S.; Tamayo, P.; Yang, W. S.; Rees, M. G.; Chen, S. X.; Boskovic, Z. V.; Javaid, S.; Huang, C.; Wu, X. Y.; Tseng, Y. Y.; Roider, E. M.; Gao, D.; Cleary, J. M.; Wolpin, B. M.; Mesirov, J. P.; Haber, D. A.; Engelman, J. A.; Boehm, J. S.; Kotz, J. D.; Hon, C. S.; Chen, Y.; Hahn, W. C.; Levesque, M. P.; Doench, J. G.; Berens, M. E.; Shamji, A. F.; Clemons, P. A.; Stockwell, B. R.; Schreiber, S. L., Dependency of a therapy-resistant state of cancer cells on a lipid peroxidase pathway. *Nature* **2017,** *547* (7664), 453-+.

4. Wang, W.; Green, M.; Choi, J. E.; Gijon, M.; Kennedy, P. D.; Johnson, J. K.; Liao, P.; Lang, X.; Kryczek, I.; Sell, A.; Xia, H.; Zhou, J.; Li, G.; Li, J.; Li, W.; Wei, S.; Vatan, L.; Zhang, H.; Szeliga, W.; Gu, W.; Liu, R.; Lawrence, T. S.; Lamb, C.; Tanno, Y.; Cieslik, M.; Stone, E.; Georgiou, G.; Chan, T. A.; Chinnaiyan, A.; Zou, W., CD8(+) T cells regulate tumour ferroptosis during cancer immunotherapy. *Nature* **2019,** *569* (7755), 270-274.

5. Jiang, X.; Stockwell, B. R.; Conrad, M., Ferroptosis: mechanisms, biology and role in disease. *Nature Reviews Molecular Cell Biology* **2021**, doi.org/10.1038/s41580-020-00324-8.

6. Yang, W. S.; SriRamaratnam, R.; Welsch, M. E.; Shimada, K.; Skouta, R.; Viswanathan, V. S.; Cheah, J. H.; Clemons, P. A.; Shamji, A. F.; Clish, C. B., Regulation of ferroptotic cancer cell death by GPX4. *Cell* **2014,** *156* (1-2), 317-331.

7. Efimova, I.; Catanzaro, E.; Van der Meeren, L.; Turubanova, V. D.; Hammad, H.; Mishchenko, T. A.; Vedunova, M. V.; Fimognari, C.; Bachert, C.; Coppieters, F.; Lefever, S.; Skirtach, A. G.; Krysko, O.; Krysko, D. V., Vaccination with early ferroptotic cancer cells induces efficient antitumor immunity. *J Immunother Cancer* **2020,** *8* (2).

8. Scheerer, P.; Borchert, A.; Krauss, N.; Wessner, H.; Gerth, C.; Höhne, W.; Kuhn, H., Structural basis for catalytic activity and enzyme polymerization of phospholipid hydroperoxide glutathione peroxidase-4 (GPx4). *Biochemistry* **2007,** *46* (31), 9041-9049.

9. Yang, W. S.; Kim, K. J.; Gaschler, M. M.; Patel, M.; Shchepinov, M. S.; Stockwell, B. R., Peroxidation of polyunsaturated fatty acids by lipoxygenases drives ferroptosis. *Proceedings of the National Academy of Sciences* **2016,** *113* (34), E4966-E4975.

10. Eaton, J. K.; Furst, L.; Ruberto, R. A.; Moosmayer, D.; Hilpmann, A.; Ryan, M. J.; Zimmermann, K.; Cai, L. L.; Niehues, M.; Badock, V., Selective covalent targeting of GPX4 using masked nitrile-oxide electrophiles. *Nature chemical biology* **2020,** *16* (5), 497-506.

11. Friedmann Angeli, J. P.; Schneider, M.; Proneth, B.; Tyurina, Y. Y.; Tyurin, V. A.;

Hammond, V. J.; Herbach, N.; Aichler, M.; Walch, A.; Eggenhofer, E.; Basavarajappa, D.; Radmark, O.; Kobayashi, S.; Seibt, T.; Beck, H.; Neff, F.; Esposito, I.; Wanke, R.; Forster, H.; Yefremova, O.; Heinrichmeyer, M.; Bornkamm, G. W.; Geissler, E. K.; Thomas, S. B.; Stockwell, B. R.; O'Donnell, V. B.; Kagan, V. E.; Schick, J. A.; Conrad, M., Inactivation of the ferroptosis regulator Gpx4 triggers acute renal failure in mice. *Nat Cell Biol* **2014,** *16* (12), 1180-91.

12. Conrad, M.; Kagan, V. E.; Bayir, H.; Pagnussat, G. C.; Head, B.; Traber, M. G.; Stockwell, B. R., Regulation of lipid peroxidation and ferroptosis in diverse species. *Gene Dev* **2018,** *32* (9-10), 602-619.

13. Jay, D. G., Selective Destruction of Protein Function by Chromophore-Assisted Laser Inactivation. *Proceedings of the National Academy of Sciences of the United States of America* **1988,** *85* (15), 5454-5458.

14. Liao, J. C.; Roider, J.; Jay, D. G., Chromophore-Assisted Laser Inactivation of Proteins Is Mediated by the Photogeneration of Free-Radicals. *Proceedings of the National Academy of Sciences of the United States of America* **1994,** *91* (7), 2659-2663.

15. Beck, S.; Sakurai, T.; Eustace, B. K.; Beste, G.; Schier, R.; Rudert, F.; Jay, D. G., Fluorophore-assisted light inactivation: A high-throughput tool for direct target validation of proteins. *Proteomics* **2002,** *2* (3), 247-255.

16. Tour, O.; Meijer, R. M.; Zacharias, D. A.; Adams, S. R.; Tsien, R. Y., Genetically targeted chromophore-assisted light inactivation. *Nature Biotechnology* **2003,** *21* (12), 1505-1508.

17. Lee, J. Y.; Udugamasooriya, D. G.; Lim, H. S.; Kodadek, T., Potent and selective photo-inactivation of proteins with peptoid-ruthenium conjugates. *Nature Chemical Biology* **2010,** *6* (4), 258-260.

18. Sato, S.; Morita, K.; Nakamura, H., Regulation of Target Protein Knockdown and Labeling Using Ligand-Directed Ru(bpy)(3) Photocatalyst. *Bioconjugate Chemistry* **2015,** *26* (2), 250-256.

19. Suzuki, A.; Tsumura, K.; Tsuzuki, T.; Matsumura, S.; Toshima, K., Target-selective degradation of proteins by a light-activated 2-phenylquinoline-estradiol hybrid. *Chemical Communications* **2007,** (41), 4260-4262.

20. Davies, M. J., Singlet oxygen-mediated damage to proteins and its consequences. *Biochem Bioph Res Co* **2003,** *305* (3), 761-770.

21. Zhang, S.; Li, Y.; Li, T.; Zhang, Y.; Li, H.; Cheng, Z.; Peng, N.; Liu, Y.; Xu, J.; He, H., Activable Targeted Protein Degradation Platform Based on Light-triggered Singlet Oxygen. *J Med Chem* **2022,** *65* (4), 3632-3643.

22. Gracanin, M.; Hawkins, C. L.; Pattison, D. I.; Davies, M. J., Singlet-oxygen-mediated amino acid and protein oxidation: Formation of tryptophan peroxides and decomposition products. *Free Radical Biology and Medicine* **2009,** *47* (1), 92-102.

23. Van Straten, D.; Mashayekhi, V.; De Bruijn, H. S.; Oliveira, S.; Robinson, D. J., Oncologic photodynamic therapy: basic principles, current clinical status and future directions. *Cancers* **2017,** *9* (2), 19, doi: 10.3390/cancers9020019.

24. Dos Santos, A. F.; Inague, A.; Arini, G. S.; Terra, L. F.; Wailemann, R. A.; Pimentel, A. C.; Yoshinaga, M. Y.; Silva, R. R.; Severino, D.; de Almeida, D. R. Q., Distinct photo-oxidation-induced cell death pathways lead to selective killing of human breast cancer cells. *Cell death & disease* **2020,** *11* (12), 1-12.

25. Donohoe, C.; Senge, M. O.; Arnaut, L. G.; Gomes-da-Silva, L. C., Cell death in

photodynamic therapy: From oxidative stress to anti-tumor immunity. *Biochimica Et Biophysica Acta-Reviews on Cancer* **2019,** *1872* (2), 188308.
26. Muchowicz, A.; Wachowska, M.; Stachura, J.; Tonecka, K.; Gabrysiak, M.; Wołosz, D.; Pilch, Z.; Kilarski, W. W.; Boon, L.; Klaus, T. J., Inhibition of lymphangiogenesis impairs antitumour effects of photodynamic therapy and checkpoint inhibitors in mice. *European Journal of Cancer* **2017,** *83*, 19-27.
27. Sakamoto, K.; Sogabe, S.; Kamada, Y.; Matsumoto, S.-i.; Kadotani, A.; Sakamoto, J.-i.; Tani, A., Discovery of GPX4 inhibitory peptides from random peptide T7 phage display and subsequent structural analysis. *Biochemical and biophysical research communications* **2017,** *482* (2), 195-201.
28. Li, C.; Deng, X. B.; Zhang, W. L.; Xie, X. W.; Conrad, M.; Liu, Y.; Angeli, J. P. F.; Lai, L. H., Novel Allosteric Activators for Ferroptosis Regulator Glutathione Peroxidase 4. *J Med Chem* **2019,** *62* (1), 266-275.
29. Doll, S.; Proneth, B.; Tyurina, Y. Y.; Panzilius, E.; Kobayashi, S.; Ingold, I.; Irmler, M.; Beckers, J.; Aichler, M.; Walch, A.; Prokisch, H.; Trumbach, D.; Mao, G. W.; Qu, F.; Bayir, H.; Fullekrug, J.; Scheel, C. H.; Wurst, W.; Schick, J. A.; Kagan, V. E.; Angeli, J. P. F.; Conrad, M., ACSL4 dictates ferroptosis sensitivity by shaping cellular lipid composition. *Nat Chem Biol* **2017,** *13* (1), 91-98.
30. Hu, Z. W.; Rao, B. Q.; Chen, S. M.; Duanmu, J., Targeting tissue factor on tumour cells and angiogenic vascular endothelial cells by factor VII-targeted verteporfin photodynamic therapy for breast cancer in vitro and in vivo in mice. *Bmc Cancer* **2010,** *10*, 235.
31. Shui, S.; Zhao, Z.; Wang, H.; Conrad, M.; Liu, G., Non-enzymatic lipid peroxidation initiated by photodynamic therapy drives a distinct ferroptosis-like cell death pathway. *Redox Biology* **2021**, DOI: 10.1016/j.redox.2021.102056.
32. Ursini, F.; Maiorino, M.; Valente, M.; Ferri, L.; Gregolin, C., Purification from pig liver of a protein which protects liposomes and biomembranes from peroxidative degradation and exhibits glutathione peroxidase activity on phosphatidylcholine hydroperoxides. *Biochimica et Biophysica Acta (BBA)-Lipids and Lipid Metabolism* **1982,** *710* (2), 197-211.
33. Ursini, F.; Maiorino, M.; Gregolin, C., The selenoenzyme phospholipid hydroperoxide glutathione peroxidase. *Biochimica et Biophysica Acta (BBA)-General Subjects* **1985,** *839* (1), 62-70.
34. Proneth, B.; Conrad, M., Ferroptosis and necroinflammation, a yet poorly explored link. *Cell Death and Differentiation* **2019,** *26* (1), 14-24.
35. van Straten, D.; Mashayekhi, V.; de Bruijn, H. S.; Oliveira, S.; Robinson, D. J., Oncologic Photodynamic Therapy: Basic Principles, Current Clinical Status and Future Directions. *Cancers* **2017,** *9* (2).
36. Alzeibak, R.; Mishchenko, T. A.; Shilyagina, N. Y.; Balalaeva, I. V.; Vedunova, M. V.; Krysko, D. V., Targeting immunogenic cancer cell death by photodynamic therapy: past, present and future. *J Immunother Cancer* **2021,** *9* (1).
37. Sakamoto, K. M.; Kim, K. B.; Kumagai, A.; Mercurio, F.; Crews, C. M.; Deshaies, R. J., Protacs: Chimeric molecules that target proteins to the Skp1–Cullin–F box complex for ubiquitination and degradation. *Proceedings of the National Academy of Sciences* **2001,** *98* (15), 8554-8559.
38. Nalawansha, D. A.; Crews, C. M., PROTACs: An Emerging Therapeutic Modality in Precision

Medicine. *Cell Chemical Biology* **2020,** *27* (8), 998-1014.
39. Gao, H. Y.; Sun, X. Y.; Rao, Y., PROTAC Technology: Opportunities and Challenges. *Acs Medicinal Chemistry Letters* **2020,** *11* (3), 237-240.